Berberine alters gut microbial function through modulation of bile acids

Patricia Wolf
University of Illinois at Chicago https://orcid.org/0000-0003-4779-7910
Saravanan Devendran
European Molecular Biology Laboratory
Heidi L. Doden
University of Illinois at Urbana-Champaign
Lindsey K. Ly
University of Illinois at Urbana-Champaign
Tyler Moore
George Mason University
Hajime Takei
Junshin Clinic Bile Acid Institute
Hiroshi Nittono
Junshin Clinic Bile Acid Institute
Tsuyoshi Murai
Health Sciences University of Hokkaido
Takao Kurosawa
Health Sciences University of Hokkaido
George E. Chlipala
University of Illinois at Chicago
Stefan J. Green
University of Illinois at Chicago
Genta Kakiyama
Virginia Commonwealth University
Purna Kashyap
Mayo Clinic Minnesota
Vance J. McCracken
Southern Illinois University Edwardsville
H. Rex Gaskins
University of Illinois at Urbana-Champaign
Patrick M. Gillevet
George Mason University
Jason M. Ridlon (jmridlon@illinois.edu)

Research article

Keywords: Berberine, bile acids, gnotobiotic mice, gut bacteria, network analysis, nutraceutical, RNA-Seq

Posted Date: June 22nd, 2020

DOI: https://doi.org/10.21203/rs.3.rs-32461/v1

Version of Record: A version of this preprint was published on January 11th, 2021. See the published version at https://doi.org/10.1186/s12866-020-02020-1.

Abstract

Background: Berberine (BBR) is a plant-based nutraceutical that has been used for millennia to treat diarrheal infections and in contemporary medicine to improve patient lipid profiles. Reduction in lipids, particularly cholesterol, is achieved partly through up-regulation of bile acid synthesis and excretion into the Gastrointestinal tract. The efficacy of BBR is also thought to be dependent on structural and functional alterations of the gut microbiome. However, knowledge of the effects of BBR on gut microbiome communities is currently lacking. Distinguishing indirect effects of BBR on bacteria through altered bile acid profiles is particularly important in understanding how dietary nutraceuticals alter the microbiome.

Results: Germfree mice were colonized with a defined minimal gut bacterial consortium capable of functional bile acid metabolism (*Bacteroides vulgatus, Bacteroides uniformis, Parabacteroides distasonis, Bilophila wadsworthia, Clostridium hylemonae, Clostridium hiranonis, Blautia producta*; B4PC2). Multi-omics (bile acid metabolomics, 16S rDNA sequencing, cecal metatranscriptomics) were performed in order to provide a simple in vivo model from which to identify network-based correlations between bile acids and bacterial transcripts in the presence and absence of dietary BBR. Significant alterations in network topology and connectedness in function were observed, despite similarity in gut microbial relative abundance between control and BBR treatment. BBR increased cecal bile acid concentrations and altered the taurocholic acid:tauro-β-muricholic acid ratio in the liver. Overall, analysis of correlation networks indicates both bacterial species-specific responses to BBR, as well as functional commonalities among species, such as up-regulation of Na^+/H^+ antiporter, cell wall synthesis/repair, carbohydrate metabolism and amino acid metabolism. Bile acid concentrations in the gastrointestinal (GI) tract increased significantly during berberine treatment and developed extensive correlation networks with expressed genes in the B4PC2 community.

Conclusions: This work has important implications for interpreting the effects of berberine on structure and function of the complex gut microbiome, which may lead to targeted pharmaceutical interventions aimed to achieve the positive physiological effects previously observed with berberine supplementation.

Background

There is considerable interest in the utilization of dietary components to modulate the gut microbiome in a manner that improves human and animal health. This is especially true of plant-based nutraceutical compounds that have been used for millennia in traditional human societies. Nutraceuticals are now being studied to determine their efficacy in microbiome-based health outcomes and their mechanism of action under controlled conditions. Berberine (BBR) is an isoquinoline alkaloid nutraceutical compound found in certain roots (*Rhizoma coptidis*) and berries (*Berberis vulgaris, Coptis chinensis*) that is traditionally utilized to treat diarrhea through its anti-microbial action [1]. Berberine also exerts lipid-lowering effects through activation of the AMP-activated protein kinase signaling pathway and increased expression of low-density lipoprotein receptor expression in the liver [2, 3]. Additionally, BBR functions to

reduce serum cholesterol by up-regulating the conversion of cholesterol into bile acids which are excreted at higher levels in feces [4, 5]. The biotransformation of BBR by gut bacteria appears to be crucial for absorption across the gut epithelium [6, 7]. Because BBR has low bioavailability outside the GI tract, the beneficial properties of BBR are thought to be due to local GI effects on the gut microbiota [6, 8, 9]. Recent reports detail alterations in gut microbiome function caused by oral BBR administration in hamsters [4], rats [8], and mice [9] including decreased taxonomic richness and enrichment of bacteria that produce short chain fatty acids. However, detailed transcriptional responses of gut bacteria to BBR treatment in vivo have yet to be reported. Moreover, since bile acids are themselves antimicrobial [10], and because bile acid concentrations are increased in response to BBR treatment, determining bile acid-dependent correlations with microbial gene expression is also important. Investigations into these responses are predicted to provide testable hypotheses that will enable future examinations of how BBR alters bacterial structure and function, and how bacteria adapt in the short-term to antimicrobial dietary compounds such as BBR, particularly in response to increased influx of intestinal bile acids.

A simple in vivo gut community model is particularly effective in measuring the effects of single dietary nutraceuticals on genome-wide microbial gene expression, particularly with microbes that are typically found in low abundance. For this we developed a microbial community modified from Narushima et al. composed of bacteria commonly found in the human GI tract that are capable of bile acid metabolism [11]. We have recently reported in vitro bile acid-induced transcriptional changes in low abundant bile acid metabolizing bacteria including *Clostridium scindens* [12], *C. hylemonae*, and *C. hiranonis* [13]. Moreover, we determined the in vivo transcriptional profile of *C. hylemonae* and *C. hiranonis* in the mouse cecum in the presence of *Bacteroides uniformis, B. vulgatus, Bilophila wadsworthia, Parabacteroides distasonis*, and *Blautia producta* [13]. We have shown that this small consortium, termed 'B4PC2', is capable of completely converting host taurine-conjugated bile acids to unconjugated bile acids and secondary bile acids such as ursodeoxycholic acid (UDCA), deoxycholic acid (DCA), and lithocholic acid (LCA). Here, we examine individual bacterial responses to BBR, and show that network correlations among host liver, cecal, and serum bile acids and bacterial transcript abundances change significantly with oral administration of BBR.

Results

Effect of berberine on global bile acid metabolome. Since previous reports have indicated that BBR affects hepatic lipids and cholesterol by increasing bile acid excretion into the large intestine [6], the global bile acid metabolome was examined in control and BBR treated gnotobiotic mice. Total liver bile acid concentrations were not significantly different between control and BBR treated mice ($P = 0.5283$) (Fig. 1A). Significant compositional differences between bile acids in BBR treated and control liver and serum were not observed; however, microbial secondary bile acid products such as deoxycholic acid (DCA), taurodeoxycholic acid (TDCA), and taurolithocholic acid (TLCA) were observed, indicating functional bile acid metabolism by the B4PC2 consortium in the GI tract (**Figure S1-S3**). By contrast, a significant increase in total cecal bile acids (4.57 ± 1.42 μmol/g vs. 1.29 ± 0.106 μmol/g; $P < 0.05$) (Fig. 1B), and cecal bile acid composition was observed after BBR treatment relative to the control

(Fig. 1C & S4). These disparate responses to BBR treatment observed in liver, serum, and cecum suggest that BBR increases fecal loss of bile acids with concomitant increased synthesis of bile acids in order to maintain baseline liver bile acid concentrations.

Functional bile acid metabolism in the cecum by the human gut B4PC2 community was evident in both control and BBR treatment groups. Deconjugation of taurine-conjugated bile acids was nearly complete. DCA and LCA, the end-products of the bile acid 7α-dehydroxylation pathway encoded by *C. hylemonae* and *C. hiranonis* [13], were major metabolites in the cecum (**Figure S4**). Conversion of CDCA to α- and β-muricholic acid (MCA) was observed (**Figure S4**); however, little conversion of MCA to murideoxycholic acid (MDCA) and ω-MCA was detected. This confirmed the mice in this study housed a microbial consortium of human bacteria, as human mixed fecal bacteria and bile acid 7α-dehydroxylating clostridia appear to be unable to metabolize MCA to MDCA and ω-MCA [11, 13–15]. Additionally, MDCA has been shown to be generated by the host [16].

Cecal composition of the B4PC2 human microbial consortium in control and berberine treated gnotobiotic mice. To determine whether the B4PC2 consortium was established in both control and BBR treated mice a microbial analysis of cecal content was performed. Sequencing of 16S rDNA resulted in 53,456 ± 3,743 reads for control ceca and 53,529 ± 3,441 reads for BBR treated ceca. Overall diversity of both control and BBR mice were consistent with the inoculated consortium indicating successful maintenance of the germ-free environment (**Figure S5**). To examine whether the composition of this bile-tolerant community is altered by BBR treatment, diversity analyses were performed on 23,900 rarefied reads from the 16S rDNA dataset. Non-metric multidimensional scaling (NMDS) and Analysis of Similarities (ANOSIM) tests of differences in beta-diversity resulted in $R = 0.141$ and $P = 0.123$ (999 permutations) indicating diversity between samples was not significant (**Figure S5**). Shannon index (alpha diversity) was not significantly different between groups ($P = 0.30$; Mann-Whitney test) (**Figure S6**). We next performed network correlation analysis on bile acids in the cecum, serum, and liver with abundances of B4PC2 consortium members. Substantial network topological changes between bile acids, and microbial taxa were observed between control and BBR networks (Fig. 2; **Supplementary Dataset 1**). These analyses indicate that the B4PC2 consortium was similarly established in control and BBR treated gnotobiotic mice, suggesting that BBR mechanisms of action are not related to composition changes in this bile acid metabolizing microbial community.

Direct effects of berberine and bile acid concentrations on gene expression by the B4PC2 consortium. Given observed topological changes between the bile acid metabolome and the B4PC2 consortium, RNA-Seq was performed on cecal content collected from control and BBR treated mice. Network correlation analyses between transcriptomic and metabolomic data were created for each member of the B4PC2 consortium in order to decern whether differences in gene expression are in response to bile acid concentration or direct effect of BBR treatment. Results for each B4PC2 member are highlighted in the following sections.

Bilophila wadsworthia. Berberine treatment resulted in significant differential expression of 123 genes (74 up-regulated; 49 down-regulated) (Fig. 3A; **Supplementary Dataset 2–4**). Transcriptome data indicate that in presence of BBR, *B. wadsworthia* imports bacterial membrane lipids (phosphatidylethanolamine) (*LadL*; 3.29 $\log_2$FC, P = 0.01), degrades ethanolamine to acetaldehyde and ammonia (ethanolamine ammonia-lyase), and converts acetaldehyde to ethanol (*adh*; 3.29 $\log_2$FC, P = 2.46E-3). High relative expression of group 1b NiFeSe hydrogenase was observed (3.56 $\log_2$FC, P = 3.66E-4), which is involved in liberation of electrons for formate, sulfite, and nitrate respiration. Pyruvate-formate lyase and formate dehydrogenase were highly expressed in *Bilophila* during BBR treatment. However, the gene most highly-expressed was nitrate reductase γ-subunit (8.04 $\log_2$FC, P = 7.07E-06). The other two most highly expressed genes were citric acid cycle enzyme malate dehydrogenase (5.43 $\log_2$FC, P = 1.04E-5) and citrate transporter (5.11 $\log_2$FC, P = 1.04E-4). Additional citric acid cycle genes and respiratory complex genes are significantly up-regulated by BBR (Fig. 3A; **Supplementary Dataset 2–4**). In addition, a gene involved in efflux of toxic substances (*matE*) was significantly up-regulated by BBR (1.72 log2FC; P = 0.01), which may indicate export of BBR by this gene product.

BBR treatment significantly affected the topology and complexity of networks between *Bilophila* gene expression and bile acid profiles in liver, serum, and cecum (Fig. 3B **& C**). Many of the gene expression networks, sparse in the control, and unconnected with bile acids, become highly interconnected during BBR treatment and relate either directly or indirectly to increased bile acid concentrations. Notably, universal stress protein (*uspA*) was highly expressed in the BBR group relative to control (3.36 $\log_2$FC; P = 0.05) as were genes involved in DNA recombination and repair (*sbcC*, *xseA*, *uvrD*). The expression of *uspA* revealed a strong positive correlation with cecal bile acids, including DCA (r = 1.0; P = 0.0), TUDCA3S (r = 0.97; P = 0.0), and MDCA (r = 0.97; P = 0.0). DCA also correlated strongly with a recently described glycyl radical enzyme (T370_R50117375; r = 1.0; P = 0.0) involved in sulfide formation from taurine (Fig. 3D) [17]. DCA and the glycyl radical enzyme shared strong positive correlation with NADH dehydrogenase subunit 1 (T370_R50109290; r = 1.0; P = 0.0) as well as direct positive correlations with glycine dehydrogenase (T370_R50113235; r = 1.0; P = 0.0). In control mice, nitrate reductase γ-subunit is positively correlated with cecal CA (r = 0.93; P = 0.001) (Fig. 3B; **Supplementary Dataset 1)**; whereas there are no direct correlations between cecal bile acids and γ-subunit in berberine treatment (Fig. 3C; **Supplementary Dataset 1)**.

Bacteroides uniformis. Seventeen genes were significantly differentially regulated in *B. uniformis* by BBR (Fig. 4A; **Supplementary Dataset 2–4**). Two genes were identified whose expression correlated to bile acids: the highly up-regulated NAD(P)H nitroreductase (ERS852554_00867; 2.49 $\log_2$FC; P = 0.02), as well as the Na^+/H^+ antiporter (1.34 $\log_2$FC; P = 0.02). A high degree of positive connectivity was observed between total cecal bile acids (r = 0.8; P = 0.046), and primary unconjugated bile acids including β-MCA (r = 0.8; P = 0.046), UCA (r = 0.87; P = 0.015) and 7-oxo-CA (r = 0.8; P = 0.046), as well as expression of acetyl-CoA carboxylase biotin carboxyl carrier protein which was induced by BBR treatment (BLV12_RS03955; 2.47 $\log_2$FC P = 4.51E-03; FDR = 0.48) (Fig. 4B **& C; Supplementary Dataset 2–4**). Chromate transporter (BLV12_RS04500; Log_2FC = 3.06; P = 0.01; FDR = 0.58) was negatively correlated with total bile acids in

the liver (r = -0.9; *P* = 0.006) and individual conjugated, sulfated, and primary bile acids (r = -0.9 to -1.0; *P* = 0.006 to *P* < 0.001).

Bacteroides vulgatus. BBR differentially altered expression of 105 genes in *B. vulgatus* (Fig. 5A; **Supplementary Dataset 2–4**). Most notably, BBR increased the expression of a polycistronic operon encoding predicted multidrug efflux pump subunits—periplasmic adaptor subunit efflux RND (3.72 log_2FC; *P* = 7.23E-08; FDR = 1.23E-05), AcrB/AcrD/AcrF (3.00 log2FC; *P* = 5.54E-07; 6.87E-05), and TolC (2.71 log_2FC; *P* = 1.6E-07; FDR = 2.26E-05). Expression of the efflux resistance-nodulation-division transporter periplasmic subunit (BVU_RS20445) was positively associated with DCA in the cecum (r = 1.0; *P* < 0.001) as well as cecal MDCA (r = 0.97; *P* = 0.0) and TUDCA-3S (r = 0.97; *P* < 0.001). In addition, a gene encoding a predicted cation/H(+) antiporter was positively correlated with total cecal bile acids (r = 1.0; *P* < 0.001) (Fig. 5B **– D; Supplementary Dataset 1**).

BBR induced increased expression of sialidase (1.44 log_2FC, *P* = 2.93E-05, FDR = 1.81E-03) and other genes involved in mucin degradation including *N*-acetylneuraminate lyase (1.33 log_2FC, *P* = 9.64E-04, FDR = 0.04), *N*-acylglucosamine 2-epimerase (1.18 log_2FC, *P* = 3.95E-08, FDR = 0.08), α-1,2-mannosidase (0.93 log_2FC, *P* = 1.64E-03 FDR = 0.05), α-L-fucosidase (0.75 log_2FC, *P* = 0.02, FDR = 0.23), and α-1,2-C3/C4-fucosidase (0.70 log_2FC; *P* = 0.02; FDR = 0.23). SusC and SusD outer membrane protein encoding genes, involved in binding and uptake of carbohydrates, were observed in the correlation network in the BBR treated group. In particular, BVU_1844 was differentially expressed in the BBR group (1.18 log_2FC; *P* = 0.03; FDR = 0.31) and negatively correlated with cecal T-β-MCA (r = -0.97; *P* < 0.001). These data may indicate a “ramping up” of carbohydrate metabolism and may explain the significant increase in total SCFA levels reported previously during BBR intake [8].

Parabacteroides distasonis. Two operons encoding predicted tryptophan (BDI_RS02910-BDI_RS02940) and leucine biosynthesis (BVU_RS10160-BVU_RS10180; BVU_RS12860-BVU_RS12880) pathways were among the most highly differentially up-regulated genes in *P. distasonis* in the presence of BBR (Fig. 6A; **Supplementary Datasets 2–4**). Genes encoding a predicted efflux RND transporter periplasmic adaptor (BDI_RS01695; 2.33 log_2FC; *P* = 1.50E-04; FDR = 0.01) and TolC (BDI_RS00690; 2.30 log_2FC; *P* = 2.04E-06; FDR = 1.37E-03) were also highly expressed, which may reflect adaptation to increased bile salt concentrations in response to BBR. Network analysis showed sparse associations between transcripts and cecal bile acids in control mouse ceca and liver (Fig. 6B **& C; Supplementary Dataset 1**), but tight interconnections between cecal and liver bile acids and transcripts after BBR treatment (Fig. 6D **& E**). While TolC expression was not correlated with cecal bile acids, efflux RND transporter had strong positive correlations with cecal DCA (r = 1.0; *P* < 0.001), TUDCA3S (r = 0.97; *P* < 0.001), and MDCA (r = 0.97; *P* < 0.001) in the BBR group (Fig. 6D). Positive correlations were also observed between cecal bile acids and genes involved in leucine and tryptophan biosynthesis (Fig. 6D). Also notable is the positive association between LCA in the cecum and the Na+/H + antiporter NhaA (BDI_R503835; 1.53 log_2FC; *P* = 4.38E-03; FDR = 0.12; r = 0.97; *P* < 0.001) (Fig. 6D). As in *B. vulgatus*, several SusC/SusD membrane associated protein genes were also differentially regulated by BBR and correlate directly or indirectly with bile acids

in the cecum and liver (Fig. 6D **& E)**. Interestingly, *P. distasonis* is observed to differentially express multidrug transporter *matE* (WP_011966429.1; 2.60 $\log_2$FC; *P* = 5.51E-05; FDR = 0.04), which does not correlate with bile acids and may indicate an export protein important for removing intracellular BBR. Indeed, MATE transporters have been shown previously to catalyze xenobiotic compound efflux in a Na + or H + dependent manner [18, 19].

Clostridium hiranonis. The most highly expressed genes in response to BBR in *C. hiranonis* were a 6 ORF polycistron encoding a helix-turn-helix xenobiotic response protein, chaperone, ATPase, ATPase, MBL fold hydrolase, and dinitrogenase iron-molybdenum cofactor (4.4 to 2.36 log2FC, *P* = 5.18E-05 to *P* = 0.024) (Fig. 7A **& B; Supplementary Dataset 2–4)**. Genes involved in peptidoglycan synthesis (*murJ* and *murF*) and maintenance of the cell-wall were also significantly up-regulated by BBR. Stress-induced genes, genes involved in DNA repair (*recN* 0.98 Log2FC; *P* = 0.021), and the exodeoxyribonuclease VII large subunit (1.19 Log2FC; *P* = 0.015) were also induced by BBR treatment (Fig. 7A). The expression of exodeoxyribonuclease VII large subunit correlated positively with DCA in the liver (r = 0.95; *P* < 0.001) and less-positive correlations were observed for other liver bile acids (MDCA, T-β-MCA, TCA, TCDCA) and negatively with 3-dehydro-4,6-CA in the control cecum (r = -0.89; *P* = 0.008) (Fig. 7C **& D; Supplementary Dataset 1)**. Expression of *recN* negatively correlated with total cecal bile acids (r = -0.89; *P* = 0.004) and σ^{54}-dependent Fis family transcriptional regulator (r = -0.9; *P* = 0.006). Interestingly, treatment with BBR changed this interaction (Fig. 7D; **Supplementary Dataset 1)**. The expression of exodeoxyribonuclease VII large subunit was not contingent on σ^{54}-dependent Fis family transcriptional regulator, but was negatively correlated with serum TCA (r = -0.86; *P* = 0.017) and total serum bile acids (r = -0.86; *P* = 0.017). Expression of σ^{54}-dependent Fis family transcriptional regulator correlated positively with liver bile acids (r = 0.8 to 1.0; *P* values from < 0.05 to < 0.001), and positively correlated with Na^+/H^+ antiporter which was itself positively correlated with CA in the liver (r = 0.8; *P* < 0.05) but negatively correlated with numerous cecal bile acids (r = -0.89 to 0.0; *P* values from 0.007 to < 0.001). It is possible that by importing protonated bile acids, it is not necessary to exchange ions and expression of the Na^+/H^+ antiporter may decrease.

A putative adhesin was also significantly expressed in the presence of BBR (2.68 Log2FC; *P* = 2.57E-03). Numerous copies of genes encoding putative cell wall-binding repeat 2 family protein were significantly down-regulated by BBR ranging from − 1.60 $\log_2$FC (FDR = 9.04E-04) to -5.59 $\log_2$FC (FDR = 7.42E-04). This may indicate modulation of the peptidoglycan layer by BBR treatment. Further support of this was the significant increase in expression of *murJ*, encoding Lipid II flippase (1.69 $\log_2$FC; *P* = 0.02; FDR = 0.16) and *murR* transcriptional regulator (1.53 $\log_2$FC; *P* = 1.90E-03; FDR = 0.04) with a trend for *murG* (1.12 $\log_2$FC; *P* = 0.10; FDR = 0.39) and *murF* (0.90 $\log_2$FC; *P* = 0.01; FDR = 0.12) was observed. Thus, *C. hiranonis* gene expression reflects responsiveness to bile acid-induced stress during BBR treatment.

Clostridium hylemonae. BBR differentially regulated 92 genes in *C. hylemonae.* Of note, a gene predicted to encode the septation ring formation regulator, EzrA, was among the most highly up-regulated genes (2.41 log2FC; *P* = 1.39E-03) (Fig. 8A; **Supplementary Dataset 2–4**), but did not correlate with cecal bile

acids. Specifically, genes involved in bile acid 7α-dehydroxylation by *C. hylemonae* were down-regulated regulated, including *baiB* encoding bile acid coenzyme A ligase (1.45 Log_2FC; *P* = 0.04), and *baiCD* encoding bile acid NAD-dependent 3-dehydro-4-oxidoreductase (-2.42 Log_2FC; *P* = 3.61E-03) (Fig. 8A). Phage genes, including holin (2.10 log_2FC; *P* = 2.8E-04) and siphovirus DUF859 (1.96 Log_2FC; *P* = 1.27E-3) as well as type I-C CRISPR Cas8c/Csd1 (1.09 log_2FC; *P* = 0.04) were up-regulated by BBR. In control mice, phage holin expression was positively correlated with cecal DCA (r = 0.81; P = 0.021), but negatively correlated with cecal T-β-MCA (r = -0.83; *P* = 0.016) and β-MCA in the liver (r = -0.94; *P* = 0.0) (Fig. 8B; **Supplementary Dataset 1**). In BBR treated mice, phage holin was positively associated with total cecal bile acids (r = 1.0; *P* = 0.0) and had a strengthened positive correlation with cecal DCA (r = 0.9; *P* = 0.006) (Fig. 8C **& D; Supplementary Dataset 1**).

Cecal RNA-Seq analysis revealed two polycistronic operons involved in the Stickland fermentation of glycine, including the glycine dehydrogenase and glycine reductase pathway genes and the formation of cofactors such as lipoate that were significantly up-regulated by BBR (Fig. 8A). In control ceca, expressed genes involved in glycine reductase (*FolD*, *grdD*) appeared to be indirectly and negatively correlated to bile acids via transcription terminator/antiterminator NusG (Fig. 8B). Lipoate-protein ligase A expression was positively correlated with expression of metabolic genes as well as CA-4,6-3-one. In BBR treated mice, lipoate-protein A displayed strong positive correlations with total cecal bile acids (r = 0.8; *P* = 0.046) and individual cecal bile acids, such as DCA (r = 0.9; *P* = 0.006) as well as weak negative correlations with liver bile acids (Fig. 8C). Positive correlations were observed between lipoate-protein ligase A and FolD, glycine cleavage protein T, and dihydrolipoyl dehydrogenase, indicating that the significant increase in glycine metabolism with BBR treatment was at least partially driven by increased bile acid concentration in the cecum.

Genes involved in sporulation in *C. hylemonae* including spore coat associated protein (*cotJA*; 2.29 log2FC; *P* = 2.89E-04), *N*-acetylmuramoyl-L-alanine amidase (*cwlD*; 1.54 log2FC; *P* = 0.03), spore germination protein (1.43 log2FC; *P* = 0.03), acid-soluble spore protein (0.96 log2FC; *P* = 0.04) were observed in response to BBR treatment. Acid-soluble spore protein was negatively correlated in control mice with liver bile acids, whereas BBR treatment resulted in a positive correlation with liver bile acids. This may indicate that up-regulation of genes involved in cell-wall maintenance and metabolism reflects the effects of both BBR and bile acids.

Discussion

BBR treatment leads to increased conversion of cholesterol into bile acids, resulting in decreased blood cholesterol levels, since bile acid synthesis is the major route of cholesterol excretion in the body [20]. These lipid lowering effects have been confirmed in a previous meta-analysis of 27 clinical trials, thus making BBR an attractive alternative for dyslipidemic patients unable to take statins [21]. However, as a nutraceutical, BBR is not regulated with the same rigor as pharmaceutical interventions. In addition, BBRs mechanism of action (increased bile acid secretion to the GI tract), is commonly associated with negative physiological effects, including increased risk of colorectal cancer [22]. This is paradoxical given that

along with demonstrated lipid lowering effects, BBR appears to exert cytotoxic effects in cancer cells [23]. Therefore, understanding BBR versus bile acid dependent effects on the gut microbiome is necessary in order to develop targeted pharmacological treatments that mimic BBRs lipid lowering outcomes. Numerous studies demonstrate that BBR alters the microbiome; however, responses of diverse commensal gut bacteria to BBR are largely unknown. The current study provides novel insight into the effects of dietary BBR on gut bacterial transcriptome profiles. This study is also the first to report effects of a changing bile acid metabolite profile on bacterial gene expression during BBR treatment. Our results are consistent with previous reports that BBR increases bile acid concentrations in the large intestine, but not the liver [6, 9, 20]. Increased bile acid concentrations in the GI tract have been reported to significantly affect the gut microbiome [22, 24]. Thus, the novel use of correlation networks to observe structural changes in transcriptome and metabolome interactions in response to BBR treatment allowed us to elucidate whether changes in gene expression were in response to increased cecal bile acid concentrations or the direct effects of BBR.

BBR feeding alters the structural composition of complex gut microbial communities potentially in response to increased colonic bile acid concentrations [6, 8, 9]. Treatment with BBR did not significantly alter the relative abundance of bacteria in the cecum of B4PC2 gnotobiotic mice. This was expected as members of the B4PC2 community are “bile-tolerant”, thus less likely to become perturbed in bile rich conditions, and growing with limited pressure for niche competition due to consortium simplicity and gnotobiotic conditions. Consequently, this provides an excellent framework by which to examine transcriptional changes of each bacteria in response to BBR treatment. Use of correlation networks to analyze transcriptomic and metabolomic changes in this minimal community allows us to determine functional changes in these bacteria that are responses to bile acid concentrations versus direct effects of BBR on member composition or abundance.

Indeed, BBR did significantly alter gut microbial-bile acid metabolite interactions (Fig. 2). For example, sulfated bile acids were positively correlated to bile acid 7α-dehydroxylating bacteria, *C. hiranonis* and *C. hylemonae*, and negatively correlated with Bacteroidetes spp. The host sulfates bile acids to act as signaling molecules, and sulfation acts as the major pathway by which humans detoxify hydrophobic bile acids [26, 27]. However, currently little is known about the effects of sulfated-bile acids on anaerobic bacterial physiology and the host. A recent report indicates that the absorption of LCA in the portal vein induces formation of cholic acid-7-sulfate (CA7S) through activation of the Vitamin D receptor [28]. CA7S was shown to be a microbiome-dependent metabolite that agonizes TGR-5 resulting in anti-diabetic effects in a bariatric surgery mouse model [28]. While we did not measure portal bile acids, LCA and its isomers were major metabolites in serum (**Figure S3**). In cecum, we found a significant increase in TUDCA3S with BBR treatment, a metabolite which correlated significantly with numerous transcripts from the B4PC2 community members. Our results indicate a potential relationship between sulfated bile acids and microbial physiological changes, although further work will be necessary to understand the role of CA3S or CA7S on host physiology.

While our study was not designed to address the metabolism of BBR in gnotobiotic mice, it was previously shown that microbial reduction of BBR to dihydroberberine by FMN-dependent nitroreductase was necessary to facilitate host BBR absorption [7]. Indeed, BBR up-regulated an FMN-dependent nitroreductase in *B. uniformis*, which may indicate metabolism of BBR by the B4PC2 community. Numerous BBR metabolites have been reported in animal models [29], and it is probable that additional anaerobic bacteria and microbial enzymes will be identified that generate BBR derivatives.

We observed a negative correlation between *B. wadsworthia* and the cecal secondary bile acids DCA and 3-oxo-DCA in control and BBR treatment, respectively. Correlations of bile acid metabolites and differential transcripts expressed by *B. wadsworthia* indicate DCA induces DNA repair and universal stress protein which controls expression of a number of genes involved in redox reactions and electron transport. In particular, a gene encoding a glycyl radical enzyme, recently reported to be involved in taurine respiration [17], was positively associated with DCA in the cecum. Interestingly, an ethanolamine degradation pathway was highly up-regulated in *B. wadsworthia* along with the nitrate reductase γ-subunit (Fig. 3D). Previous metabolomic studies of BBR and oryzanol demonstrated a significant increase in fecal ethanolamine with 4-week treatment of 150 mg kg^{-1} BBR [30]. Phosphotidylethanolamine is the primary membrane lipid in bacteria [31] and gut microbes have evolved complex pathways to metabolize this compound. The antimicrobial nature of BBR leads to lysis and release of bacterial membrane components as evidenced by prior descriptions of reduced total microbial load by BBR [8], and reports that BBR inhibits the cell division protein FtsZ thus leading to cell death [32, 33]. Metatranscriptomic analysis indicates that *B. wadsworthia* up-regulates a lipid transporter (LadL) and genes predicted to encode enzymes involved in ethanolamine utilization. Utilization of bacterial phosphatidylethanolamine would yield ATP by substrate-level phosphorylation from acetyl-phosphate [31]. Additionally, genes encoding enzymes in the citric acid cycle and the electron transport chain were up-regulated, which may indicate that *B. wadsworthia* converts bacterial fatty acids to acetyl-CoA via anaerobic respiration, with nitrate and taurine serving as terminal electron acceptors. Nitrate reductase induction is intriguing since other pathobionts such as enterohemorrhagic *E. coli* utilize host nitrosative respiratory bursts for anaerobic respiration [34]. These results indicate that increased concentration of secondary bile acids due to BBR treatment induces the stress response in *Bilophila*, and that BBR may directly affect microbial physiology through alteration of growth substrates and terminal electron acceptors used in anaerobic respiration.

There were several important observations made with respect to the effect of BBR on *C. hylemonae*. First, numerous cell wall and membrane architecture genes were differentially regulated (Fig. 8D). In particular, the regulator of septation ring formation, EzrA, was significantly up-regulated by BBR. Previous work in *E. coli* demonstrated that BBR inhibits GTPase activity and destabilizes septation ring protofilaments [32]. This indicates that BBR may affect microbial growth through targeting EzrA in both gram-negative and gram-positive bacteria inhabiting the GI tract [33]. Importantly, EzrA transcripts were not observed to correlate with bile acid metabolites, suggesting that inhibition of EzrA gene expression may be directly due to BBR treatment as seen in *E. coli.* By contrast, BBR treatment led to a tight clustering of cecal bile

acids to phage holin in *C. hylemonae* (Fig. 8C), suggesting that BBR-induced alterations in the gut microbiome observed in complex consortia may be partly due to induction of the phage lytic cycle through bile acid toxicity. Indeed, previous studies have shown that bile acids induce phage lytic cycle in intestinal pathogens [35, 36].

Na+/H + antiporter was up-regulated by BBR and highly correlated with cecal bile acids in *C. hylemonae*, *C. hiranonis*, *B. uniformis, P. distasonis*, and *B. vulgatus*. This is consistent with previous reports of bile resistance by the multi-subunit Na+/H + antiporter in *Bacillus subtilis* [37] and *Vibrio cholera* [38]. Thus, the process by which BBR alters the gut microbiome is likely partly due to its choleretic effects. Previous studies in which bile acids were fed to rodents, and thus enriched in the GI tract, demonstrate the role bile acids play in structuring the gut microbiome via anti-microbial selection pressure [24].

Conclusions

The current study indicates that BBR has both bile acid-dependent and independent effects on the B4PC2 consortium related to stress response, bile and xenobiotic tolerance, and changes in energy metabolism. These responses observed in a defined human gut consortium in gnotobiotic mice are critical to elucidate the effects of BBR supplementation on complex gut microbial communities. The implications of this research are increased understanding of altered microbial function in response to BBR versus increased GI concentrations of bile acid, which may lead to targeted pharmaceutical interventions that mimic the positive effects observed with supplementation of the nutraceutical BBR.

Methods

Bacterial strains and chemical reagents

The B4PC2 consortium consisted of *Bacteroides uniformis* ATCC 8492, *Bacteroides vulgatus* ATCC 8482, *Clostridium hylemonae* DSM 15053, *Clostridium hiranonis* DSM 13275, *Parabacteroides distasonis* DSM 20701, *Bilophila wadsworthia* DSM 11045, and *Blautia producta* ATCC 27340. Strains were cultured and stored as previously described [13]. Authentic reference bile acids were described in our recent publication [13] and purchased from Sigma-Aldrich (St. Louis, MO) and internal standards were obtained from C/D/N Isotopes (Pointe-Claire, QC, Canada). Rare bile acids and sulfated-derivatives were gifts from Professor Iida, Nihon University, Tokyo, Japan (takaiiada@chs.nihon-u.ac.jp). Solvents (water, ethanol, methanol, acetonitrile) were of high-performance liquid chromatography grade, and ammonium acetate was analytical grade, all of which were purchased from Kanto Chemical (Tokyo, Japan). An InertSep C18-B (100 mg/ml) solid phase extraction cartridge was obtained from GL Sciences (Tokyo, Japan).

Gnotobiotic Mice

All experiments were completed following guidelines of the Institutional Animal Care and Use Committees of the Mayo Clinic (Rochester, MN) (Protocol# A00001902-16). Mice were provided ad libitum access to autoclaved LabDiet 5K67 through wire bar feeders. Ad libitum access to autoclaved water was provided

by means of polysulfone bottles with a shoulder hole. Six-week old C57BL/6N mice (*N* = 12) were purchased from Taconic Farms (Germantown, NY), randomly separated into two isolators and orally gavaged with 200 µl of glycerol stock (33% v/v) containing ~ 10^8 CFU of each member of the B4PC2 consortium. From day 14–27, mice were gavaged daily with either sterile saline, or berberine (100 mg kg^{-1} final). Berberine for oral gavage (25 mg/ml) was suspended in PBS containing 0.5% carboxymethylcellulose to maintain solubility. On day 27, mice were euthanized by CO_2 asphyxiation followed by cervical dislocation. Serum, liver, and cecal contents and tissues were stored at -80°C for subsequent bile acid analysis. A separate portion of cecal contents was snap frozen and stored at -80° C for microbial community analysis.

Microbiome Community Profiling

Genomic DNA was extracted from cecum samples using a Maxwell® 16 Tissue DNA Purification Kit, with extractions conducted on a Maxwell16 automated extraction system (Promega, Madison, WI, USA). Library preparation, pooling, and MiniSeq sequencing were performed at the DNA Services facility, Research Resources Center, University of Illinois at Chicago as described previously [13]. Gnomic DNA was PCR amplified with primers 515F-modified and 926R [39] targeting the V4-V5 variable region of the microbial small subunit ribosomal RNA gene using a two-stage “targeted amplicon sequencing” protocol [40, 41]. The primers contained 5' common sequence tags (known as common sequence 1 and 2, CS1 and CS2) [42]. First and second stage PCR amplifications were performed in 10 microliter reactions in 96-well plates, using the MyTaq HS 2X mastermix (Bioline, Taunton, MA), and PCR conditions as recently described. Pooled libraries were purified with an AMPure XP cleanup protocol, spiked with phiX, and subjected to MiniSeq sequencing to obtain 2 × 150 bp paired-end reads. Forward and reverse reads were merged using PEAR [43] and trimmed based on a quality threshold of p = 0.01. Ambiguous nucleotides and primer sequences were removed and sequences less than 300 bp were discarded. Chimeric sequences were identified and removed using the USEARCH algorithm with a comparison to GreenGenes 13_8. [44, 45]. Resulting sequence files were merged with sample information and operational taxonomic unit clusters were generated in QIIME using the UCLUST algorithm with a 97% similarity threshold [46, 47]. Taxonomic annotations for each OTU were determined using the UCLUST algorithm and GreenGenes 13_8 reference with a minimum similarity threshold of 90% [44, 45].

Cecal RNA-Seq analysis. Extraction, library preparation and sequencing were performed at the DNA Services facility, Research Resources Center, University of Illinois at Chicago, as previously described [13]. Total RNA was extracted from mouse cecum using an EZ1 RNA tissue kit (Qiagen, Germantown, MD), and conducted on an EZ1 automated extraction instrument [13]. Prior to extraction, tissue was homogenized with a FastPrep-24 5G bead-beating device (MP Biomedicals) at 6 m/s for 40 sec. Additional DNase treatment of total RNA extracts were performed using the RNeasy Mini Kit (Qiagen) based on the RNeasy Total RNA Cleanup Protocol (W.M. Keck, Foundation Biotechnology Resource Laboratory at Yale University). Two hundred and fifty ng of total RNA was subjected to ribosomal RNA depletion using both mouse and bacterial Ribo-Zero rRNA Removal Kit (Illumina, San Diego, CA) according to the

manufacturer's instructions. The resulting double depleted RNA was used as input for ScriptSeq library preparation according to the manufacturer's instructions. ScriptSeq v2 RNA-Seq Library Prep kit (Illumina) was utilized to generate cecal mRNA-Seq libraries. Resulting libraries were pooled and sequenced on an Illumina NextSeq500 instrument using paired-end 2 × 150 base reads. Bioinformatics of RNA-Seq datasets was performed as previously described [13]. Raw RNA-seq reads with Q scores < 32 were aligned with Ribosomal RNA sequences prepared from the B4PC2 genomes using bowtie2 (v2.3.3.1). HTSeq (v0.9.1) counting was performed in union mode against Gene Feature Format annotations of the B4PC2 genomes. Reads were counted against coding DNA sequences of each bacterium. Differential gene expression analysis between BBR treatment and control was performed using edgeR [47] and limma [48] R packages, with a minimum *P*-value of < 0.05 accepted as indicating differentially expressed genes. Genes were binned according to known functionality, and category analysis was performed using eggNOG [49].

Sample preparation for bile acid metabolomics. Bile acid sample preparation and LC-MS/MS for bile acid analysis were essentially based on the previously developed method and was performed after extraction from samples as previously described [13, 50]. In short, cecum contents were lyophilized and 90% ethanol (2 ml) was added to 10 mg of the dried matter. For liver, 300–400 mg of sample was homogenized with cold water (500 µl) and 20 mg/ml of Proteinase K solution, and digested at 55 °C for 16 h. Bile acids were extracted from dried cecal content and homogenized liver three times by ultra-sonication at room temperature for 1 h. Supernatant was separated by centrifugation at 2,500 rpm for 5 min after each ultra-sonication cycle and combined into a glass test tube. Liver and cecal samples were then evaporated to dryness under an N_2 stream. Serum (50 µl) was added to acetonitrile (5 ml) and was also evaporated to dryness. Prepared crude bile acid extracts were then re-suspended in 90% ethanol (1 ml) by ultra-sonication and, deuterium-labeled internal standards, d_4-CA, d_4-GCA and d_4-TCA were added at each concentration at 100 nmol/ml. An aliquot (100 µl) was diluted with water (900 µl) and then applied to a solid-phase extraction cartridge (InertSep C18-B 100 mg sorbent weight, pre-conditioned with 1 ml of methanol and 3 ml of water). The column was washed with water (1 ml) and then desired bile acids were eluted with 90% ethanol (1 ml). After evaporation of the solvent, the residue was dissolved in 20% acetonitrile (1 ml), and aliquot (5 µl) of the solution was analyzed by the LC/ESI-MS/MS.

LC/ESI-MS/MS analysis. The LC/ESI-MS/MS system comprised a LCMS-8050 tandem mass spectrometer, equipped with an ESI probe and Nexera X2 ultra high-pressure liquid chromatography system (Shimadzu, Japan). A separation column, InertSustain C18 (150 mm × 2.1 mm ID, 3 µm particle size; GL Sciences Inc., Tokyo, Japan), was employed at 40 °C. A mixture of 10 mM ammonium acetate and acetonitrile was used as the eluent, and the separation carried out by linear gradient elution at a flow rate of 0.2 ml/min. Mobile phase, LC parameters and MS parameters were the same as recently reported [13].

Network Correlation Analysis. Correlation network analysis [51] and Correlation Difference Network analysis were performed for cecal transcriptomics and bile acid metabolomics from serum, liver, and cecum. Data were combined into a single feature table and Spearman correlations were calculated

between all features using a custom Python program and P values were calculated as described previously [52]. A PERL script was used to filter the correlations based on a defined Rho (i.e. $r > 0.7$) and a defined P-values (i.e. $P > 0.001$). Networks were plotted in Cytoscape to visualize the statistically significant correlations and these are used to develop hypotheses about the interactions between the features [53]. We then used a custom Python program to calculate correlation differences [54] between the feature pairs; that is correlations that have significantly changed between the two treatments. This allows inferences of interactions that have changed between the control and BBR treatment identifying key metabolic shifts induced by BBR. The Correlation Network and Correlation Difference tools are deployed on our Galaxy Portal (http://mbac.gmu.edu:8080).

Accession numbers. Cecal RNA-Seq datasets were deposited as Bioproject PRJNA523415.

List Of Abbreviations

Berberine (BBR), *Bacteroides vulgatus, Bacteroides uniformis. Bilophila wadsworthia, Blautia producta, Parabacteroides distasonis, Clostridium hylemonae, Clostridium hiranonis* (B4PC2 consortium), phosphate buffered saline (PBS), colony forming units (CFU), targeted amplicon sequencing (TAS), non-metric multidimensional scaling (NMDS), analysis of similarities (ANOSIM), Taurocholic acid (TCA), cholic acid (CA), 3-sulfoglycocholic acid (GCA3S), 3-sulfotaurocholic acid (TCA3S), 3-sulfoCA (CA3S), glycochenodeoxycholic acid (GCDCA), taurochenodeoxycholic acid (TCDCA), chenodeoxycholic acid (CDCA), 3-sulfoglycochenodeoxycholic acid (GCDCA3S), 3-sulfo-taurochenodeoxycholic acid (TCDCA3S), 3-sulfochenodeoxycholic acid (CDCA3S), glycoursodeoxycholic acid (GUDCA), tauroursodeoxycholic acid (TUDCA), ursodeoxycholic acid (UDCA), 3-sulfoglycoursodeoxycholic acid (GUDCA3S), 3-sulfotauroursodeoxycholic acid (TUDCA3S), 3-sulfoursodeoxycholic acid (UDCA3S), glycodeoxycholic acid (GDCA), taurodeoxycholic acid (TDCA), deoxycholic acid (DCA), 3-sulfoglycodeoxycholic acid (GDCA3S), 3-sulfotaurodeoxycholic acid (TDCA3S), 3-sulfodeoxycholic acid (DCA3S), gastrointestinal (GI), glycolithocholic acid (GLCA), taurolithocholic acid (TLCA), lithocholic acid (LCA), 3-sulfoglycolithocholic acid (GLCA3S), 3-sulfotaurolithocholic acid (TLC3S), 3-sulfolithocholic acid (LCA3S), glycohyocholic acid (GHCA), taurohyocholic acid (THCA), hyocholic acid (HCA), norcholic acid (nor-CA), murocholic acid (MCA), tauro-α-murocholic acid (T-α-MCA), α-murocholic acid (α-MCA), tauro-α-murocholic acid 3-sulfate (T-α-MCA-3S), α-murocholic acid 3-sulfate (α-MCA-3S) tauro-β-murocholic acid (T-β-MCA), β-murocholic acid (β-MCA), tauro-β-murocholic acid 3-sulfate (T-β-MCA-3S), β-murocholic acid 3-sulfate (β-MCA-3S), tauro-w-murocholic acid (T-β-MCA), murodeoxycholic acid (MDCA), glycohyodeoxycholic acid (GHDCA), taurohyodeoxycholic acid (THDCA), hyodeoxycholic acid (HDCA), iso-cholic acid (iso-CA), 3-oxo-cholic acid (3-oxo-CA), 7-oxo-deoxycholic acid (7-oxo-DCA), 12-oxo-chenodeoxycholic acid (12-oxo-LCA), isochenodeoxycholic acid (iso-CDCA), 3-oxo-chenodeoxycholic acid (3-oxo-CDCA), 7-oxolithocholic acid (7-oxo-LCA), ursocholic acid (UCA), iso-deoxycholic acid (iso-DCA), 3-oxo-deoxycholic acid (3-oxo-DCA), iso-lithocholic acid (iso-LCA), allo-iso-lithocholic acid (allo-iso-LCA).

Declarations

Ethics approval and consent to participate: All experiments were completed following guidelines of the Institutional Animal Care and Use Committees of the Mayo Clinic (Rochester, MN) (Protocol# A00001902-16).

Consent for publication: Not applicable

Availability of data and material: All data generated or analyzed during this study are included in this published article [and its supplementary information files]. Cecal RNA-Seq datasets were deposited as Bioproject PRJNA523415.

Competing interests: All authors have consented to this manuscript and have no conflicts of interest to declare.

Funding: We gratefully acknowledge the financial support provided to J.M.R. for new faculty startup through the Department of Animal Sciences at the University of Illinois at Urbana-Champaign (grant Hatch ILLU-538-916) as well as Illinois Campus Research Board RB18068 (cost of gnotobiotics). This work was also supported by grants (JMR, HRG) 1RO1 CA204808-01, NIH R01CA179243, College of ACES 2017 FIRE grant (JMR, HRG) and the Young Investigators Grant for Probiotic Research (JMR; Danone, Yakult) (cost of multi-omics), as well as a grant through the Illinois-Mayo Alliance (JMR) (cost of gnotobiotics). L.L. is supported by a Graduate Research Fellowship through the National Science Foundation. P.G.W is supported by the UIC Cancer Education and Career Development Training Program Administered by the Institute for Health Research and Policy at the University of Illinois at Chicago with funding by the National Cancer Institute (Grant No. T32CA057699)

Authors' contributions: All authors have read and approved the manuscript. J.M.R., P.M.G., H.R.G., and V.J.M., conceived of the experiments; P.G.W., S.D., H.L.D., L.K.L, J.M.R., P.K., V.J.M. performed experiments; H.T., H.N., T.M.2 (Tsuyoshi Murai), T.K., G.K., performed metabolomics analysis; S.J.G, G.E.C., performed sequencing and provided datasets; S.D., J.M.R., P.G.W., H.L.D, L.K.L, T.M.1 (Tyler Moore), P.M.G., analyzed datasets; J.M.R., P.G.W., V.J.M., H.R.G, wrote and edited the manuscript. J.M.R., funded the experiments.

Acknowledgements: Not applicable

References

1. Menees S, Saad R, Chey WD. Agents that act luminally to treat diarrhea and constipation. Nat Rev Gastroenterol Hepatol. 2012;9(11):661–74.
2. Lee YS, Kim WS, Kim KH, Yoon MJ, Cho HJ, Shen Y, Ye JM, Lee CH, Oh WK, Hohnen-Behrens C, Gosby A, Kraegen EW, James DE, Kim JB. Berberine, a natural plant product, activates AMP-activated protein kinase with beneficial metabolic effects in diabetic and insulin-resistant states. Diabetes. 2006;55(8):2256–64.
3. Brusq JM, Ancellin N, Grondin P, Guillard R, Martin S, Saintillan Y, Issandou M. Inhibition of lipid synthesis through activation of AMP kinase: An additional mechanism for the hypolipidemic effects

of berberine. J Lipid Res. 2006;47:1281–88.

4. Gu S, Cao B, Sun R, Tang Y, Paletta JL, Wu X, Liu L, Zha W, Zhao C, Li Y, Ridlon JM, Hylemon PB, Zhou H, Aa J, Wang G. A metabolomic and pharmacokinetic study on the mechanism underlying the lipid-lowering effect of orally administered berberine. Mol Biosyst. 2015;11:463–74.
5. Wang Y, Yi X, Ghanam K, Zhang S, Zhao T, Zhu X. Berberine decreases cholesterol levels in rats through multiple mechanisms, including inhibition of cholesterol absorption. Metabolism. 2014;63:1167–77.
6. Pan GY, Wang GJ, Liu XD, Fawcett JP, Xie YY. The involvement of P-glycoprotein in berberine absorption. Pharmacol Toxicol. 2002;91:193–7.
7. Feng R, Shou JW, Zhao ZX, He CY, Ma C, Huang M, Fu J, Tan XS, Li XY, Wen BY, Chen X, Yang XY, Ren G, Lin Y, Chen Y, You XF, Wang Y, Jiang JD. Transforming berberine into its intestine-absorbable form by the gut microbiota. Sci Rep. 2015;5:12155.
8. Zhang X, Zhao Y, Zhang M, Pang X, Xu J, Kang C, Li M, Zhang C, Zhang Z, Zhang Y, Li X, Ning G, Zhao L. Structural changes of gut microbiota during berberine-mediated prevention of obesity and insulin resistance in high-fat diet-fed rats. PLoS ONE. 2012;7(8):e42529.
9. Guo Y, Zhang Y, Huang W, Selwyn FP, Klaassen CD. Dose-response effect of berberine on bile acid profile and gut microbiota in mice. BMC Compl Alt Med. 2016;16:394.
10. Watanabe M, Fukiya S, Yokota A. Comprehensive evaluation of the bactericidal activities of free bile acids in the large intestine of humans and rodents. J Lipid Res. 2017;58(6):1143–52.
11. Narushima S, Itoha K, Miyamoto Y, Park SH, Nagata K, Kuruma K, Uchida K. Deoxycholic acid formation in gnotobiotic mice associated with human intestinal bacteria. Lipids. 2006;41(9):835–43.
12. Devendran S, Shrestha R, Alves JMP, Wolf PG, Ly L, Hernandez AG, Mendez C, Inboden A, Wiley J, Paul O, Allen A, Springer E, Wright CL, Fields CJ, Daniel SL, Ridlon JM. ClostridiumscindensATCC 35704: Integration of nutritional requirements, the complete genome sequence, and global transcriptional responses to bile acids. ApplEnvironMicrobiol 2019; 2019; 85(7). pii: e00052-19.
13. Ridlon JM, Devendran S, Alves JMP, Doden H, Wolf PG, Ly L, Volland A, Muto A, Takei H, Nittono H, Murai T, Kurosawa T, Chlipala GE, Green SJ, Kakiyama G, Cann I, Kashyap P, McCracken V, Gaskins HR. **The 'in vivo lifestyle' of bile acid 7α**-dehydroxylating bacteria: Comparative genomics, metatranscriptomics and bile acid metabolomics analysis of a defined microbial community in gnotobiotic mice. Gut Microbes. 2020;11(3):381–404.
14. Ridlon JM, Harris SC, Bhowmilk S, Kang DJ, Hylemon PB. Consequences of bile salt metabolism by intestinal bacteria. Gut Microbes. 2016;7(1):22–39.
15. Marion S, Studer N, Desharnais L, Menin L, Escrig S, Meibom A, Hapfelmeier S, Bernier-Latmani R. In vitro and in vivo characterization of *Clostridium scindens* bile acid transformations. Gut Microbes 2018: 1–23.
16. Chiang JY. Bile acids: regulation of synthesis. J Lipid Res. 2009;50:1955–66.
17. Peck SC, Denger K, Burrichter A, Irwin SM, Balskus EP, Schleheck D. A glycyl radical enzyme enables hydrogen sulfide production by the human intestinal bacterium *Bilophila wadsworthia*. Proc Natl

Acad Sci USA. 2019;116(8):3171–6.

18. Thanassi DG, Cheng LW, Nikaido H. Active efflux of bile salts by *Escherichia coli*. J Bacteriol. 1997;179(8):2512–8.
19. Kuroda T, Tsuchiya T. Multidrug efflux transporters in the MATE family. Biochim Biophys Acta. 2009;1794(5):763–8.
20. Sun R, Yang N, Kong B, Cao B, Feng D, Yu X, Ge C, Huang J, Shen J, Wang P, Feng S, Fei F, Guo J, He J, Aa N, Chen Q, Pan Y, Schumacher JD, Yang CS, Guo GL, Aa J, Wang G. Orally Administered Berberine Modulates Hepatic Lipid Metabolism by Altering Microbial Bile Acid Metabolism and the Intestinal FXR Signaling Pathway. Mol Pharmacol. 2017;91(2):110–22.
21. Lan J, Zhao Y, Dong F, Yan Z, Zheng W, Fan J, Sun G. Meta-analysis of the effect and safety of berberine in the treatment of type 2 diabetes mellitus, hyperlipemia and hypertension. J Ethnopharmacol. 2015;161:69–81.
22. Ridlon JM, Wolf PG, Gaskins HR. Taurocholic acid metabolism by gut microbes and colon cancer. Gut Microbes. 2016;22:1–15.
23. Guamán Ortiz LM, Lombardi P, Tillhon M, Scovassi AI. Berberine, an Epiphany Against Cancer. Molecules. 2014;19:12349–67.
24. Islam KB, Fukiya S, Hagio M, Fujii N, Ishizuka S, Ooka T, Ogura Y, Hayashi T, Yokota A. Bile acid is a host factor that regulates the composition of the cecal microbiota in rats. Gastroenterology. 2011;141(5):1773–81.
25. Inagaki T, Moschetta A, Lee YK, Peng L, Zhao G, Downes M, Yu RT, Shelton JM, Richardson JA, Repa JJ, Mangelsdorf DJ, Kliewer SA. Regulation of antibacterial defense in the small intestine by the nuclear bile acid receptor. Proc Natl Acad Sci USA. 2006;103(10):3920–5.
26. Hylemon PB, Zhou H, Pandak WM, Ren S, Gil G, Dent P. Bile acids as regulatory molecules. J Lipid Res. 2009;50(8):1509–20.
27. Alnouti Y. Bile acid sulfation: a pathway of bile acid elimination and detoxification. Toxicol Sci. 2009;108:225–46.
28. Chaudhri SN, Harris DA, Henke MT, Vernon AH, Tavakkoli A, Sheu EG, Devlin AS. Bariatric surgery increases levels of a gut-restricted TGR-5 agonist that exhibits anti-diabetic effects. bioRxiv.
29. Xu P, Xu C, Li X, Li D, Li Y, Jiang J, Yang P, Duan G. Rapid Identification of Berberine Metabolites in Rat Plasma by UHPLC-Q-TOF-MS. Molecules 2019;24(10).
30. Li M, Shu X, Xu H, Zhang C, Yang L, Zhang L, Ji G. Integrative analysis of metabolome and gut microbiota in diet-induced hyperlipidemic rats treated with berberine compounds. J Transl Med. 2016;14(1):237.
31. Kaval KG, Garsin DA. Ethanolamine Utilization in Bacteria. MBio 2018; 9(1). pii: e00066-18.
32. Domadia PN, Bhunia A, Sivaraman J, Swarup S, Dasgupta D. Berberine targets assembly of *Escherichia coli* cell division protein FtsZ. Biochemistry. 2008;47(10):3225–34.

33. Singh JK, Makde RD, Kumar V, Panda D. A membrane protein, EzrA, regulates assembly dynamics of FtsZ by interacting with the C-terminal tail of FtsZ. Biochemistry. 2007;46(38):11013–22.
34. Winter SE, Winter MG, Xavier MN, Thiennimitr P, Poon V, Keestra AM, Laughlin RC, Gomez G, Wu J, Lawhon SD, Popova IE, Parikh SJ, Adams LG, Tsolis RM, Stewart VJ, Bäumler AJ. Host-derived nitrate boosts growth of *E. coli* in the inflamed gut. Science. 2013;339:708–11.
35. Kim S, Ryu K, Biswas, Ahn J. Survival, prophage induction, and invasive properties of lysogenic *Salmonella* Typhimurium exposed to simulated gastrointestinal conditions. Arch Microbiol. 2014;196:655–9.
36. Yasugi M, Okuzaki D, Kuwana R, Takamatsu H, Fujita M, Sarker MR, Miyake M. Transcriptional Profile during Deoxycholate-Induced Sporulation in a *Clostridium perfringens* Isolate Causing Foodborne Illness. Appl Environ Microbiol. 2016;82(10):2929–42.
37. Ito M, Guffanti AA, Oudega B, Krulwich TA. *mrp*, a multigene, multifunctional locus in *Bacillus subtilis* with roles in resistance to cholate and to Na^+ and in pH homeostasis. *J Bacteriol* 1999;181:2394–2402.
38. Dzioba-Winogrodzki J, Winogrodzki O, Krulwich TA, Boin MA, Hase CC, Dibrov P. The *Vibrio cholerae* Mrp system: cation/proton antiport properties and enhancement of bile salt resistance in a heterologous host. J Mol Microbiol Biotechnol. 2009;16:176–86.
39. Walters W, Hyde ER, Berg-Lyons D, Ackermann G, Humphrey G, Parada A, Gilbert JA, Jansson JK, Caporaso JG, Fuhrman JA, Apprill A, Knight R. Improved bacterial16S rRNA gene (V4 and V4-5) and fungal internal transcribed spacer marker gene primers for microbial community surveys. mSystems 2015; 1(1). pii: e00009-15.
40. Green SJ, Venkatramanan R, Naqib A. Deconstructing the polymerase chain reaction: Understanding and correcting bias associated with primer degeneracies and primer-template mismatches. PLoS One. 2015;10(5):e0128122.
41. Bybee SM, Bracken-Grissom H, Haynes BD, Hermansen RA, Byers RL, Clement MJ, Udall JA, Wilcox ER, Crandall KA. Targeted amplicon sequencing (TAS): A scalable next-gen approach to multilocus, multitaxa phylogenetics. Genome Biol Evol. 2011;3:1312–23.
42. Moonsamy PV, Williams T, Bonella P, Holcomb CL, Höglund BN, Hillman G, Goodridge D, Turenchalk GS, Blake LA, Daigle DA, Simen BB, Hamilton A, May AP, Erlich HA. High throughput HLA genotyping using 454 sequencing and the Fluidigm Access Array™ System for simplified amplicon library preparation. Tissue Antigens. 2013;81(3):141–9.
43. Zhang J, Kobert K, Flouri T, Stamatakis A. PEAR: A Fast and Accurate Illumina Paired-End ReAd MergeR. Bioinformatics. 2014;30(5):614–20.
44. Edgar RC. 2010. Search and Clustering Orders of Magnitude Faster than BLAST. Bioinformatics 2010; 26(19):2460–2461.
45. McDonald D, Morgan NP, Goodrich J, Nawrocki EP, DeSantis TZ, Probst A, Andersen GL, Knight R, Hugenholtz P. An Improved Greengenes Taxonomy with Explicit Ranks for Ecological and Evolutionary Analyses of Bacteria and Archaea. ISME J. 2012;6(3):610–8.

46. Caporaso JG, Kuczynski J, Stombaugh J, Bittinger K, Bushman FD, Costello EK, Fierer N, Peña AG, Goodrich JK, Gordon JI, Huttley GA, Kelley ST, Knights D, Koenig JE, Ley RE, Lozupone CA, McDonald D, Muegge BD, Pirrung M, Reeder J, Sevinsky JR, Turnbaugh PJ, Walters WA, Widmann J, Yatsunenko T, Zaneveld J, Knight R. QIIME allows analysis of high-throughput community sequencing data. Nat Methods. 2010;7(5):335–6.
47. Robinson MD, McCarthy DJ, Smyth GK. edgeR: a Bioconductor package for differential expression analysis of digital gene expression data. Bioinformatics. 2010;26(1):139–40.
48. Ritchie ME, Phipson B, Wu D, Hu Y, Law CW, Shi W, Smyth GK. limma powers differential expression analyses for RNA-sequencing and microarray studies. Nucleic Acids Res. 2015;43(7):e47.
49. Huerta-Cepas J, Szklarczyk D, Heller D, Hernandez-Plaza A, Forslund SK, Cook H, Mende DR, Letunic I, Rattei T, Jensen LJ, von Mering C, Bork P. eggNOG 5.0: a hierarchical, functionally and phylogenetically annotated orthology resource based on 5090 organisms and 2502 viruses. Nucleic Acids Res. 2019;47(D1):D309–14.
50. Kakiyama G, Muto A, Takei H, Nittono H, Murai T, Kurosawa T, Hofmann AF, Pandak WM, Bajaj JS. A simple and accurate HPLC method for fecal bile acid profile in healthy and cirrhotic subjects: Validation by GC-MS and LC-MS. J Lipid Res. 2014;55(5):978–90.
51. Naqvi A, Rangwala H, Keshavarzian A, Gillevet P. Network-based modeling of the human gut microbiome. Chem Biodivers. 2010;7(5):1040–50.
52. Morgenthal K, Weckwerth W, Steur R. Metabolomic networks in plants: Transitions from pattern recognition to biological interpretation. BioSystems. 2006;83:108–17.
53. Shannon P, Markiel A, Ozier O, Baliga NS, Wang JT, Ramage D, Amin N, Schwikowski B, Ideker T. Cytoscape: a software environment for integrated models of biomolecular interaction networks. Genome Res. 2003;13(11):2498–504.
54. Weckwerth W, Loureiro M, Wenzel K, Fiehn O. Differential metabolic networks unravel the effects of silent plant phenotypes. Proc. Natl. Acad. Sci. USA 2004; 101:7809–7814.

Supplementary Materials

Figure S1. Profile of liver bile acids from control and berberine treated mice.

Figure S2. Profile of three most abundant liver bile acids from control and berberine treated mice.

Figure S3. Serum bile acid profile in control and berberine treated mice.

Figure S4. Profile of cecal bile acids between control and berberine treated mice not represented in Figure 1. Significance determined by student *t* test. * $P < 0.05$.

Figure S5: 16S rDNA profile of human gut bacterial consortium in cecal samples of gnotobiotic fed control diet versus berberine. A. Relative abundance of bacterial families in control mice (C1-C6) and

berberine treatment (B1-B6) B. Non-metric multidimensional scaling (NMDS) plot of beta diversity based on Bray-Curtis index. ANOSIM test results: $R = 0.141$, $P = 0.123$, 999 permutations.

Figure S6. Shannon Index comparison between control mice and berberine treatment. The rarified 23,900 MiSeq dataset was used. Mann-Whitney test $P = 0.309$.

Supplementary Dataset 1: Correlation Networks

Supplementary Dataset 2: RNA-Seq Control Ceca

Supplementary Dataset 3: RNA-Seq Berberine Ceca

Supplementary Dataset 4: Fold Change Statistics

Figures

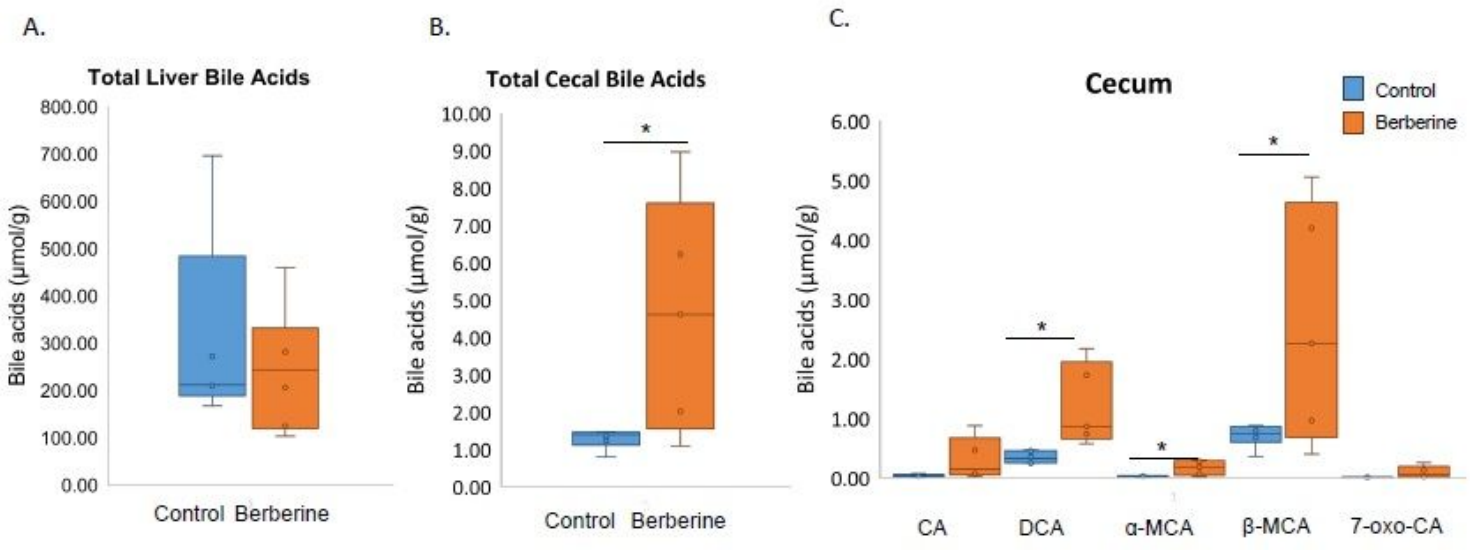

Figure 1

Berberine increases cecal total bile acids and deoxycholic acid. A. Box-plot of total bile acids in the liver between control and berberine-treated mice. B. Total bile acids in cecum between control and berberine-treated mice. C. Selected bile acids in cecum between control and berberine-treated mice. P<0.05 (*).

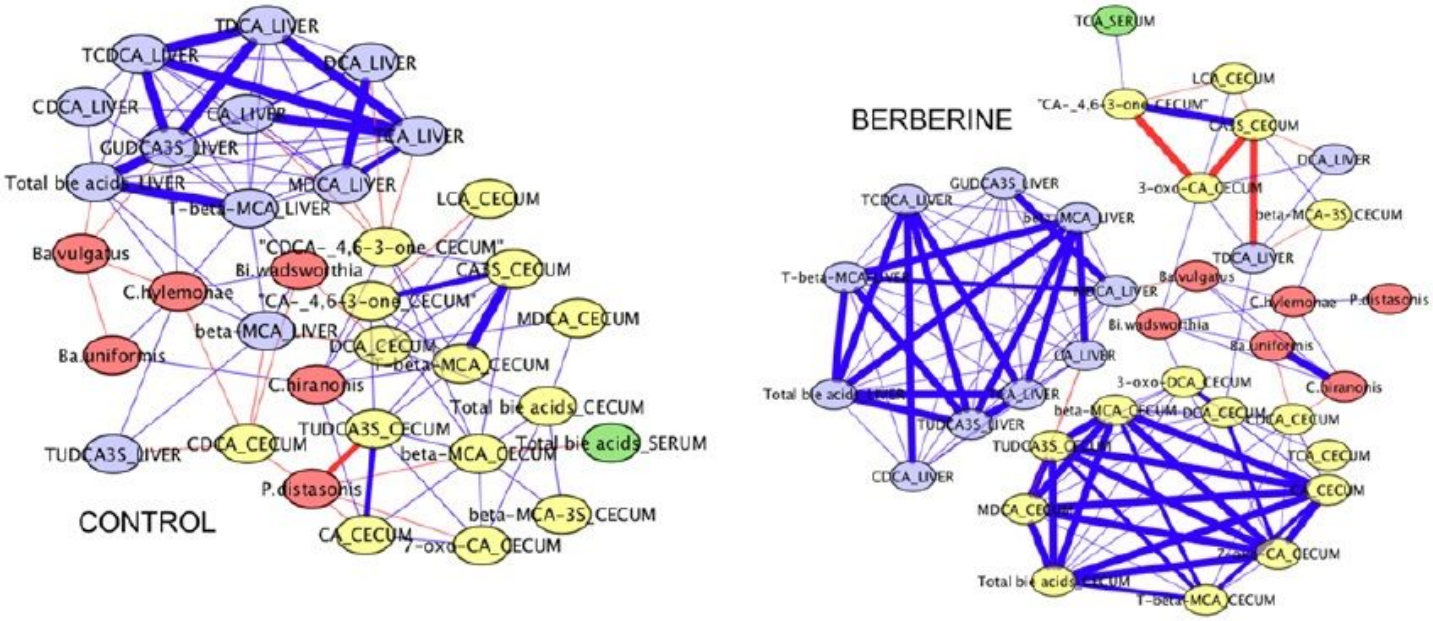

Figure 2

Network interactions between bacterial taxa in the cecum and bile acids in the liver, serum, and cecum on control diet and berberine treatment. Nodes are as follows: Liver bile acids (blue ovals), cecal bile acids (yellow ovals), cecal bacteria (red ovals).

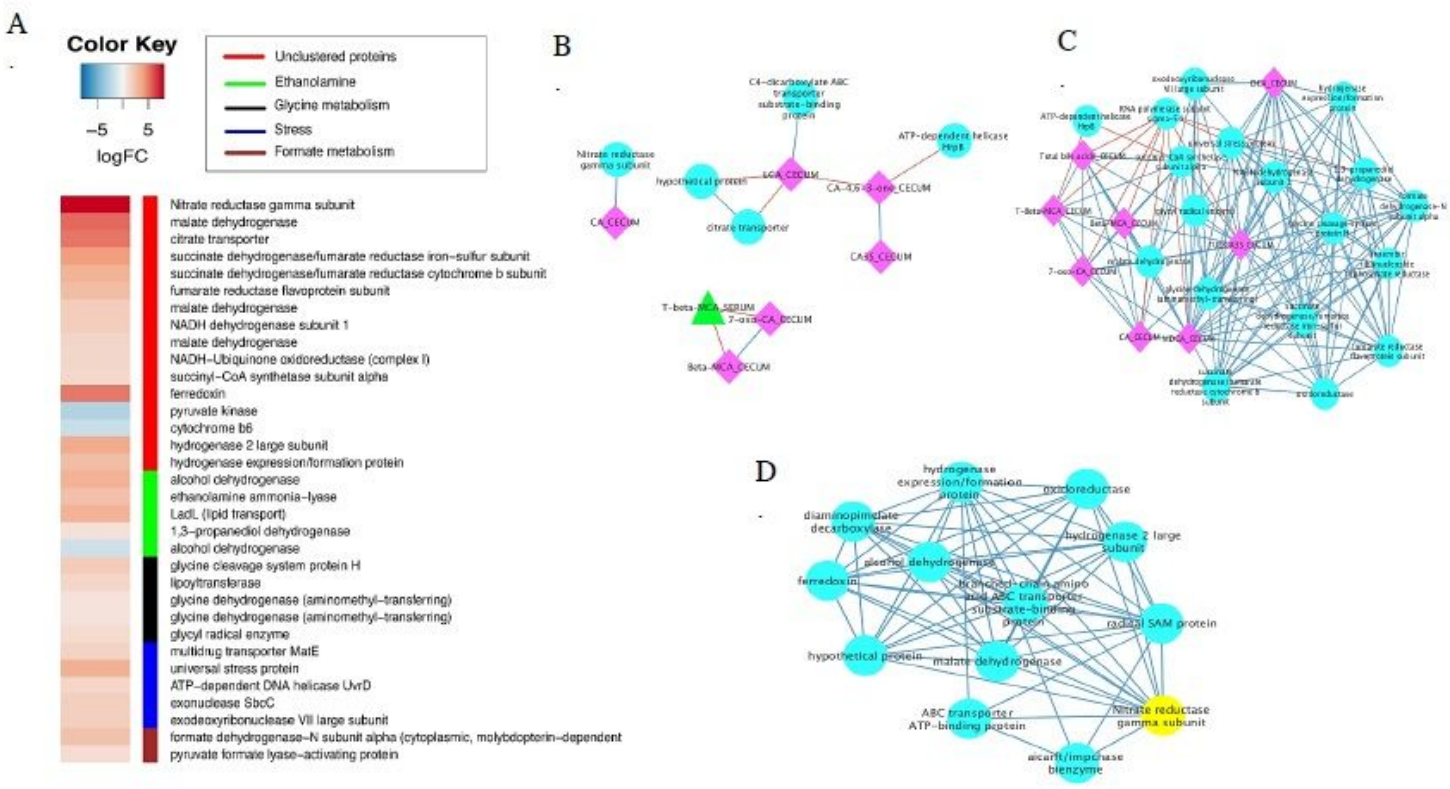

Figure 3

Effect of berberine on Bilophila wadsworthia on in vivo gene expression and network interactions. A. Heat map of differential gene expression (log2FC >(-)0.58; P < 0.05) for B. wadsworthia grouped by function. B. Network interactions between B. wadsworthia cecal gene expression and bile acid profile from cecum, liver, and serum in control group. C. Network interactions between B. wadsworthia cecal gene expression and bile acid profile from cecum, liver, and serum in berberine-treated group. D. Sub-network showing interactions between DCA in the cecum and gene expression as well as gene expression interaction with nitrate reductase. Data points with Spearman correlations < 0.7 and a P values < 0.05 are displayed.

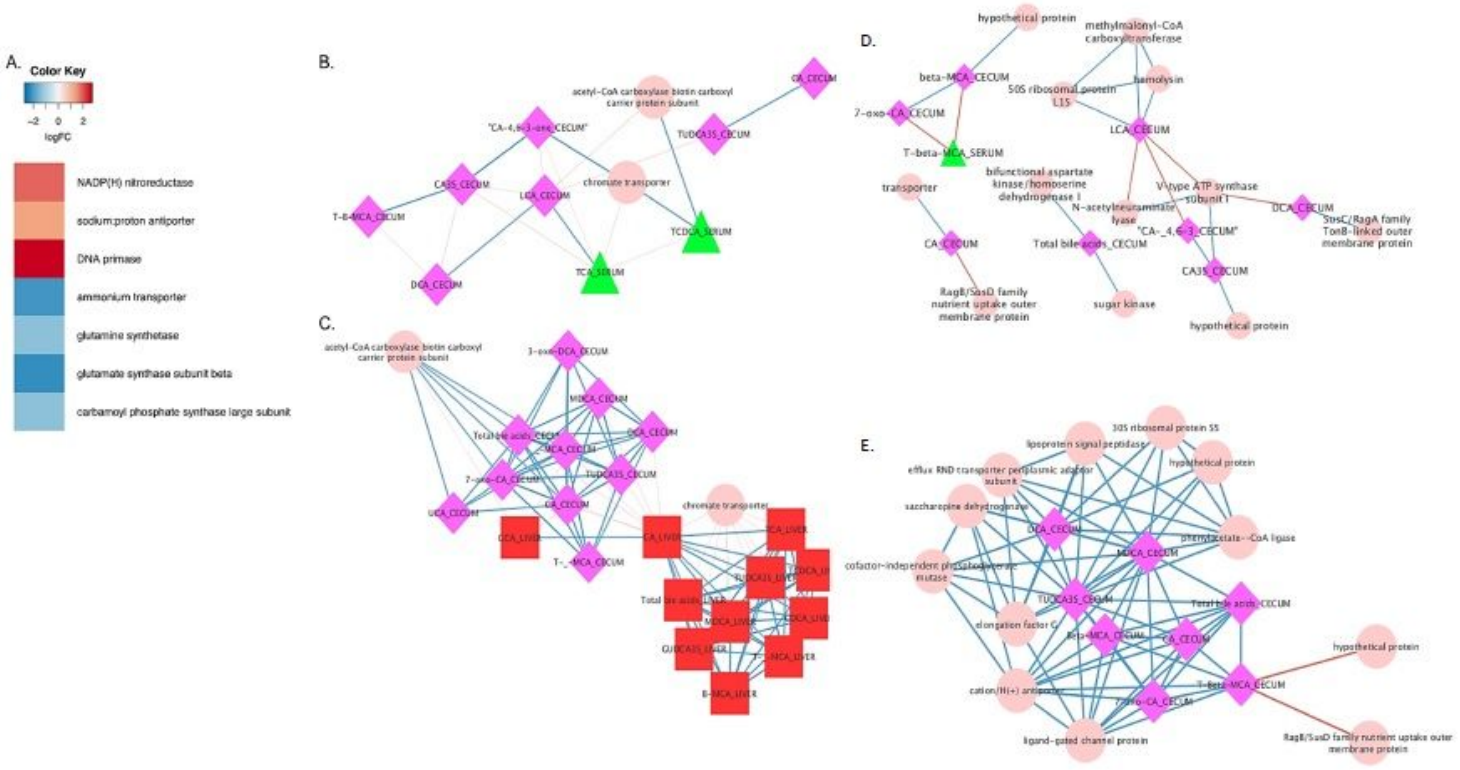

Figure 4

Response of Bacteroides uniformis to berberine treatment. A. Heat map of differentially expressed genes (log2FC >(-)0.58; P < 0.05) by B. uniformis. B. Network interactions in control mice. C. network interactions in berberine-treated mice. Nodes are as follows: bacterial genes expressed (pink circles), cecal bile acids (fuschia squares) and serum bile acids (green triangles). Data points with Spearman's correlations < 0.7 and a P values < 0.05 are displayed.

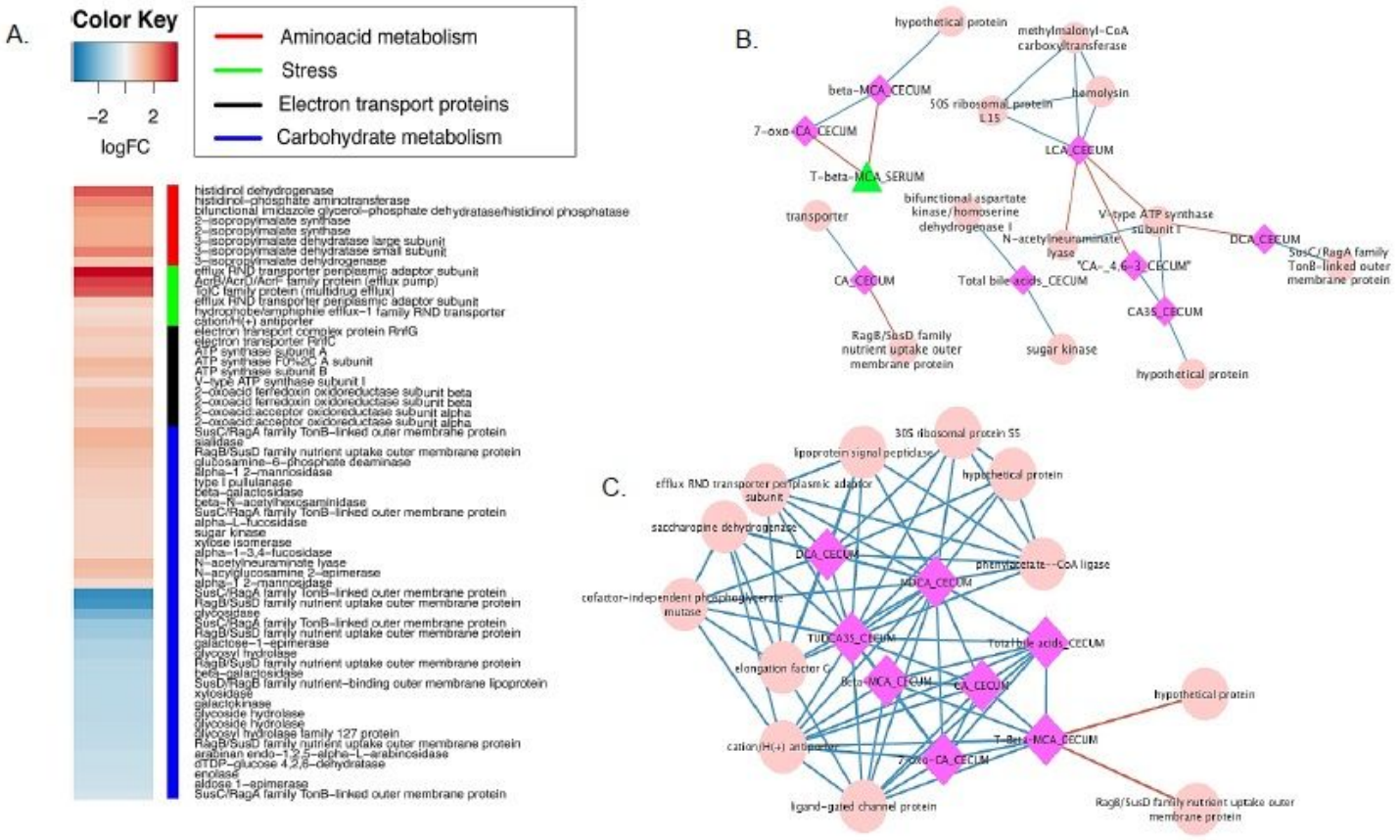

Figure 5

Network analysis of Bacteroides vulgatus response to berberine. A. Heat map of differentially expressed genes (log2FC >(-)0.58; P < 0.05) by B. vulgatus. B. Network interactions in control mice. C. Network interactions in berberine-treated mice. D. Sub-network of interactions with DCA in the cecum. Nodes are as follows: bacterial gene expression (pink circles), liver bile acids (red squares), serum bile acids (green triangles), cecal bile acids (fuschia squares). Data points with Spearman's correlations < 0.7 and a P values < 0.05 are displayed.

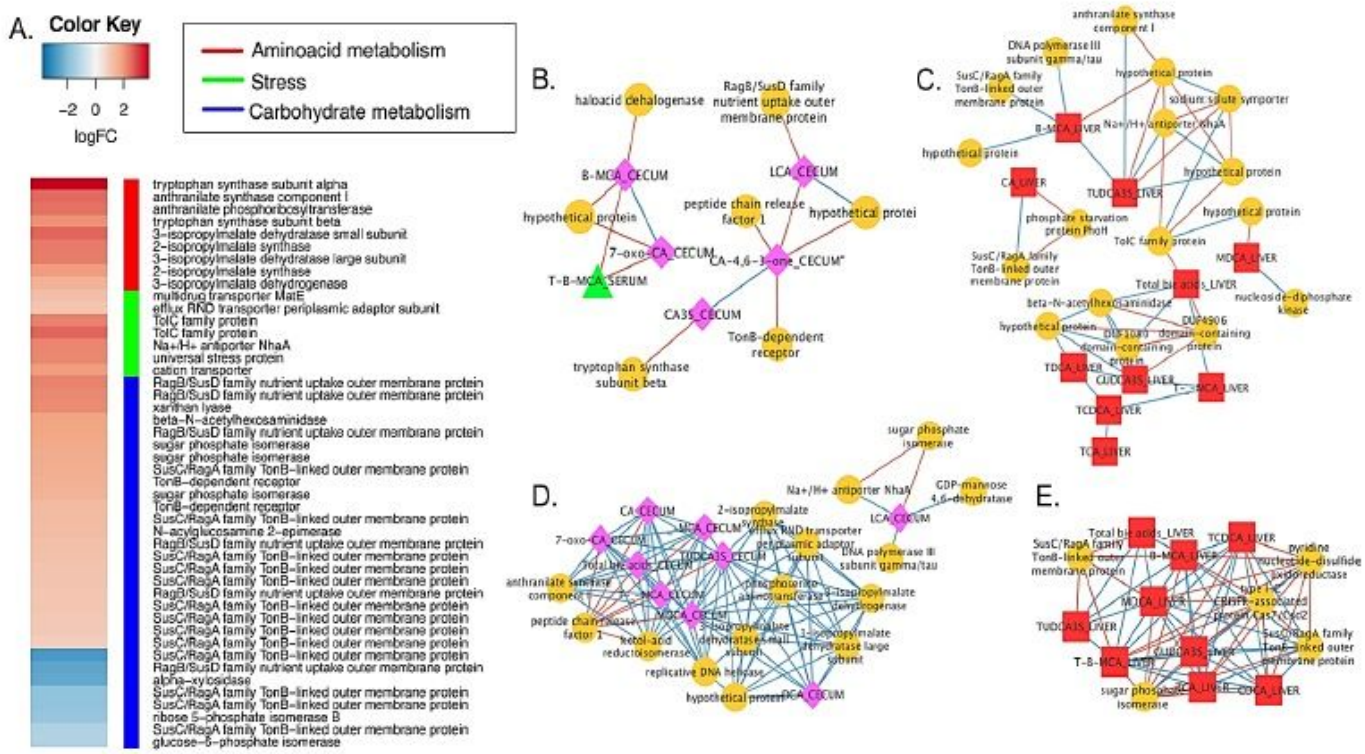

Figure 6

Effect of berberine on P. distasonis gene expression-bile acid network interactions. A. Heat map of differentially expressed genes (log2FC >(-)0.58; P < 0.05) by P. distasonis in the mouse cecum between control diet and berberine treatment. B. Network of cecal bile acid (pink diamonds), serum bile acids (green triangle), and cecal bacterial gene expression (orange circules) in control ceca. C. Correlations between liver bile acids (red squares) and cecal gene expression in control ceca. D. Network of cecal bile acids, serum bile acids, cecal bacterial gene expression in mouse berberine-treated ceca. E. Correlations between liver bile acids and cecal gene expression during berberine-treatment. Data points with Spearman's correlations < 0.7 and a P values < 0.05 are displayed.

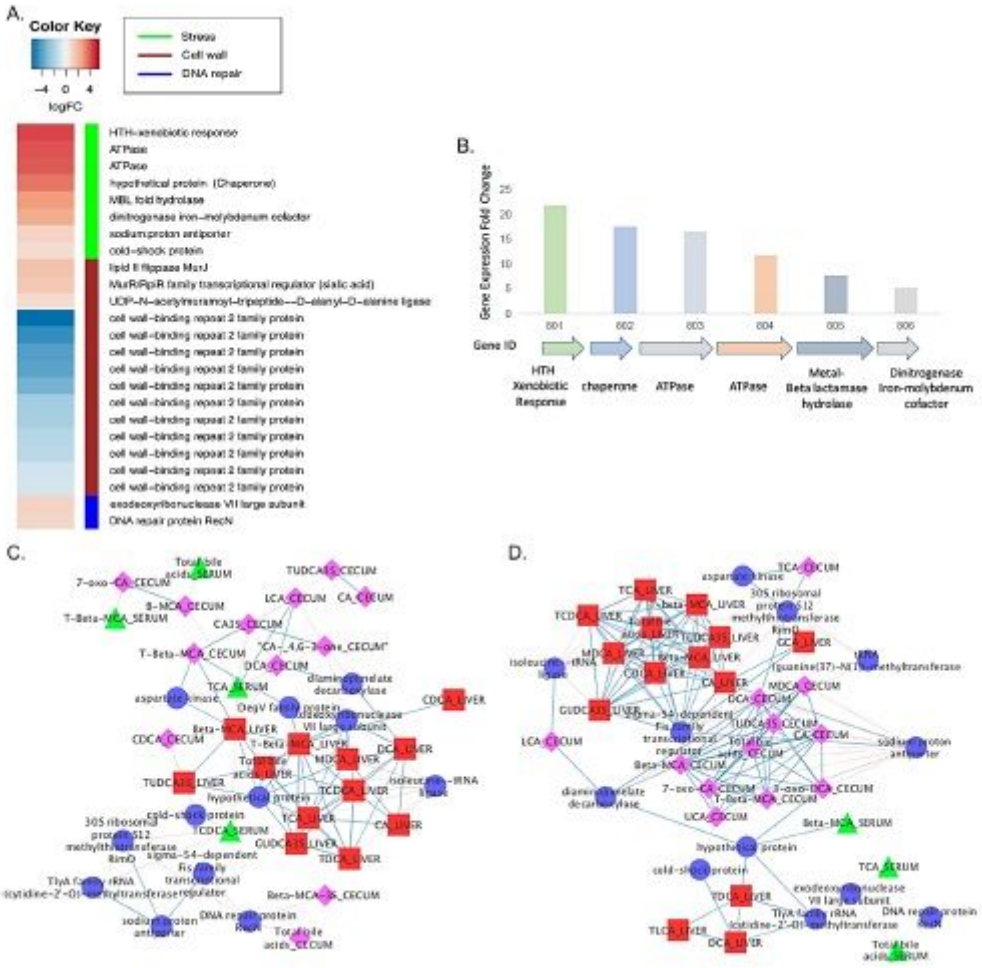

Figure 7

Clostridium hiranonis expresses a gene cluster encoding a xenobiotic response transcription factor during berberine treatment. A. Heat map of differentially expressed genes (log2FC >(-)0.58; P < 0.05) by C. hiranonis in the mouse cecum between control diet and berberine treatment. B. Organization and gene fold change of a gene cluster highly upregulated by berberine. C. Network displaying interactions between expressed genes and bile acid metabolome in control mice. D. Network displaying interactions between expressed genes and bile acid metabolome in berberine-treated mice. Data points with Spearman's correlations < 0.7 and a P values < 0.05 are displayed.

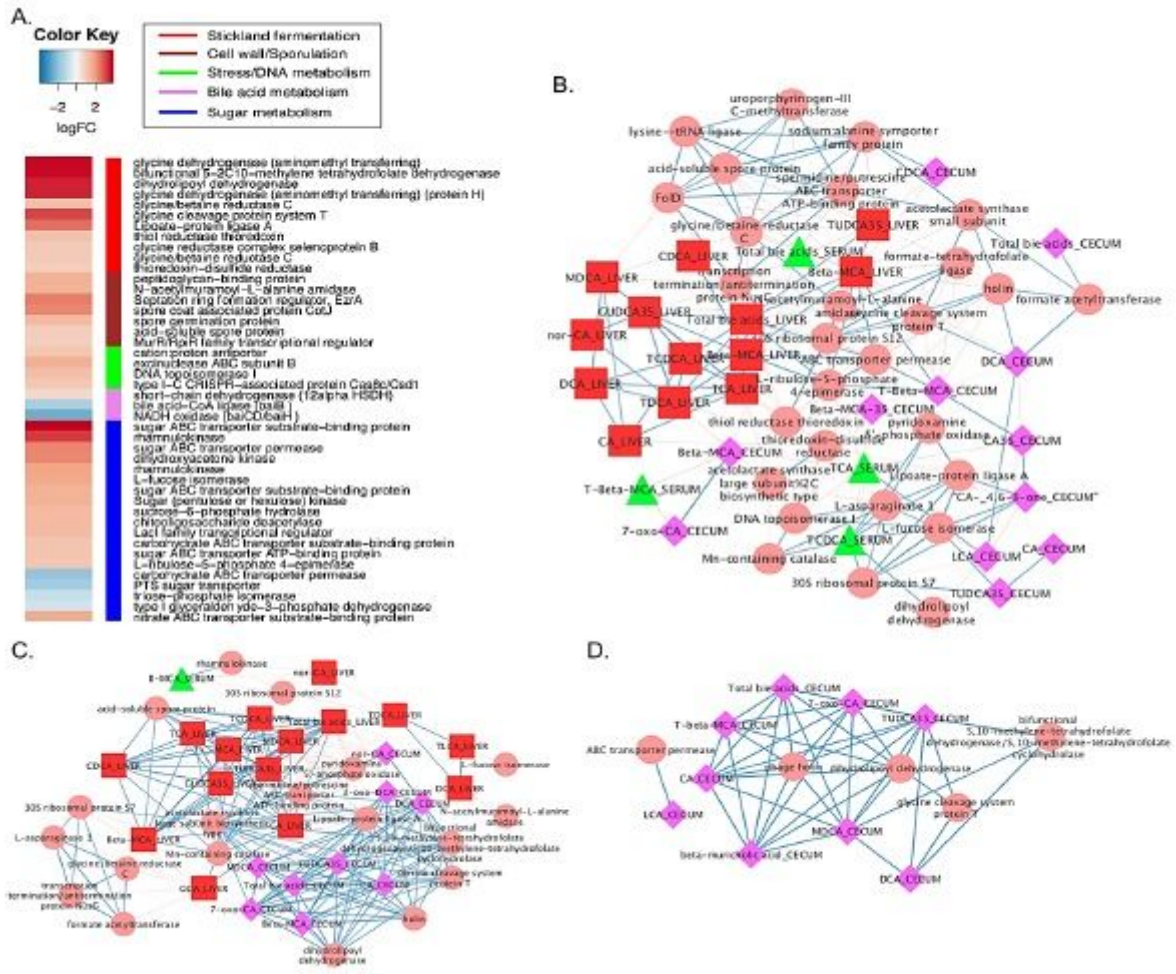

Figure 8

Network analysis between cecal gene expression by Clostridium hylemonae and bile acid metabolome. A. Heat map of differentially expressed genes (log2FC >(-)0.58; P < 0.05) by C. hiranonis in the mouse cecum between control diet and berberine treatment. B. Network displaying interactions between expressed genes and bile acid metabolome in control mice. C. Network displaying interactions between expressed genes and bile acid metabolome in berberine-treated mice. D. Sub-network of cecal bile acid-gene expression network from berberine-treated mice. Data points with Spearman's correlations < 0.7 and a P values < 0.05 are displayed.

Supplementary Files

This is a list of supplementary files associated with this preprint. Click to download.

- CopyofSupplementaryDataset4FoldChangeStatistics.xlsx
- NC3RsARRIVEGuidelinesChecklistPWPagenumbers.pdf
- S1.pdf

- SupplementaryDataset2RNASeqControlData.xlsx
- SupplementaryDataset3RNASeqBerberineData.xlsx
- SupplementaryDatasetCorrelationNetworks.xlsx
- S2.pdf
- S3.pdf
- S4.pdf
- S5.pdf
- S6.pdf